Three-dimensional laser-induced fluorescence measurements in a helicon plasma

R. Hardin, X. Sun, and E. E. Scime[a)]
Department of Physics, West Virginia University, Morgantown, West Virginia 26506-6315

(Presented on 21 April 2004; published 12 October 2004)

We describe a three-dimensional (3D) laser-induced fluorescence (LIF) diagnostic for argon ions in a helicon plasma source. With three different laser injection orientations at a single spatial location, LIF measurements are performed to determine the 3D ion temperature and the 3D ion flow vector. The measurement process is then repeated at multiple locations in a cross section of the plasma column to create a two-dimensional (2D) map of the 3D ion flow, the ion temperature, and metastable ion density. Scanning in the 2D plane is accomplished by mounting the injection and collection optics on stepping motor driven stages.
 [DOI: 10.1063/1.1787168]

I. INTRODUCTION

Laser-induced fluorescence (LIF) in plasmas provides nonperturbative, spatially resolved, measurements of particle (ion or atom) velocity distribution functions.[1] LIF has been used in many types of plasma discharges, including helicon plasma sources, to measure ion flow, ion temperature, magnetic field strength, and plasma density.[2–7] Typically, these measurements are made at a single location in a plasma. Some research groups have performed planar LIF measurements in which a laser beam is spread into a sheet and used to illuminate a cross section of a plasma.[8,9] The induced fluorescence is then imaged with a camera and a two-dimensional (2D) image of LIF intensity and flow along the direction of the laser beam obtained. If the laser has a narrow enough linewidth, such diagnostic approaches can even provide spatially resolved measurements of ion temperature[8] without perturbing the plasma as occurs when arrays of probes are used to measure plasma density, plasma flow, or magnetic fluctuations throughout a plasma cross section.[10,11] Measurements of two ion velocity components using multiplex LIF at a single location have also been previously reported.[12] In this work, we describe a LIF diagnostic capable of measuring ion flow and ion temperature in all three Cartesian directions throughout a cross section of a cylindrical helicon plasma source. The LIF measurements of the complete ion flow field enable us to determine the radial diffusion of the ions and, along with a 2D model of ion flow in a cylindrical plasma, to estimate the steady-state electric field profile.

II. APPARATUS

The hot helicon experiment (HELIX) vacuum chamber Fig.1 is a 61 cm long, Pyrex tube 10 cm in diameter connected to a 91 cm long stainless-steel chamber that is 15 cm in diameter. The stainless-steel chamber has one set of four 6 in. Conflat™ crossing ports in the center of the chamber and two sets of four 2¾ in. Conflat™ crossing ports on either side that are used for LIF diagnostic access. The opposite end of the stainless-steel chamber opens into a 2 m diameter space chamber, the Large Experiment on Instabilities and Anisotropies (LEIA).[13] Ten electromagnets produce a steady-state axial magnetic field of 0–1200 G in the source. The source gas is argon at neutral pressures of 1–10 mTorr. A precision mass flow controller regulates the argon, helium, or mixed gas flow rate. During operation, the neutral pressure in LEIA ranges from four to ten times lower than the pressure in the plasma source. rf power of up to 2.0 kW over a frequency range of 6–18 MHz is used to create the steady-state plasma. A 19 cm, half-wave, right-handed helix antenna is used to generate the plasma. The right-handedness is relative to the magnetic field direction, and is designed to launch the $m=+1$ helicon wave toward LEIA. A common electrical ground is used for the vacuum chambers and the rf amplifier. All plasma potential measurements are referenced to the chamber potential. Characteristic electron temperature and densities in the steady state-plasma are $T_e \approx 4$ eV and $n \geqslant 1 \times 10^{13}$ cm^3 as measured with a rf compensated Langmuir probe.[14] For the measurements reported here, the magnetic field in LEIA was fixed at 35 G.

In a typical LIF measurement, the frequency of a very narrow bandwidth laser is swept across a collection of ions or atoms that have a thermally broadened velocity distribution. The atoms or ions absorb a photon when it is at the appropriate frequency in its rest frame. After a short time, depending on the lifetime of the excited state, the atom or ion emits a photon of either the same frequency or another frequency. Measurement of the intensity of the emitted photons as a function of laser frequency constitutes a LIF measurement. Our LIF laser system consists of a 6 W Coherent Innova 300 argon-ion laser that pumps a Coherent 899 tunable ring dye laser tuned to 611.49 nm. The 611.49 nm (air wavelength) photons pump the Ar-II $3d^2G_{9/2}$ metastable state to the $4p^2F_{7/2}$ state that then decays to the $4s^2D_{5/2}$ state by emitting 460.96 nm photons. A mechanical chopper is used to modulate the typically 150 mW laser beam at 2 kHz be-

a)Electronic mail: escime@wvu.edu

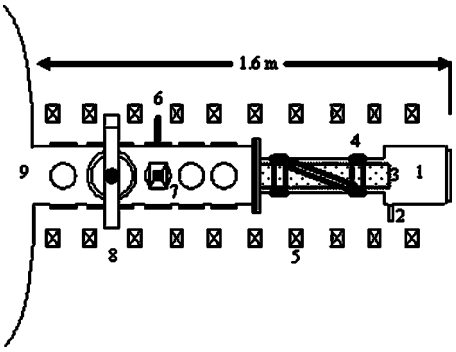

FIG. 1. Schematic view of the HELIX plasma source: (1) Pumping station, (2) gas inlet, (3) plasma column, (4) fractional helix antenna, (5) magnetic field coils, (6) retractable RF compensated Langmuir probe, (7) microwave interferometer, (8) LIF injection and collection optics and (9) space chamber.

fore it is coupled into a multimode, nonpolarization preserving, fiber optic cable. The fiber optic cable transports the laser light from the laser laboratory to the helicon source. As the laser frequency is varied over 20 GHz, the fluorescent emission from the pumped upper level is collected and transported via fiber optic cable to a filtered (1 nm bandwidth around 461 nm) narrowband, high-gain, Hamamatsu photomultiplier tube (PMT). The PMT signal is composed of fluorescence radiation, electron-impact-induced radiation, and electronic noise. A Stanford Research SR830 lock-in amplifier is used to eliminate all signals not correlated with the laser modulation. Lock-in amplification is indispensable since the electron-impact-induced emission is several orders of magnitude larger than the fluorescence signal. 10% of the laser output is passed through an iodine cell for a consistent zero-velocity reference measurement and to compensate for laser drift. Fluorescent emission from the iodine cell is detected with a photodiode for each scan of the dye laser wavelength.

The LIF collection and injection optics for perpendicular (to the magnetic field) measurements are mounted on two independent, but coupled, computer-controlled, Velmex™ stepping motor stages located as shown in Fig. 1. The collection optics (Fig. 2) consist of a multimode fiber cable coupled to a 2.54 cm outer diameter (o.d.) collimating lens with a matching numerical aperture (NA) (NA=0.22) to maximize light collection from the collection lens. The 2.54 cm o.d. collection lens is mounted in front of the collimating lens and the waist of the collection spot is 0.075 cm at the

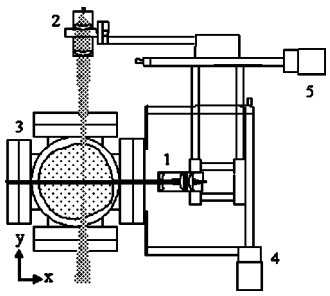

FIG. 2. The 2D scanning apparatus: (1) Beam reducing and polarizing injection optics, (2) optimized collection optics, (3) plasma source chamber, (4) *Y*-axis scanning stage, and (5) *X*-axis scanning stage.

location of the injected laser beam. The injection optics consist of another 2.54 cm o.d. collimating lens, followed by a linear polarizer with its polarization axis aligned along the magnetic field, and a beam reducing Galilean telescope. The less than 50 mW collimated injection beam has a diameter of 0.5 ± 0.05 cm across the entire plasma column. When the LIF interrogation volume ($\sim 3.9\times10^{-3}$ cm^3) is scanned in the vertical direction, both the injection and collection optics move as a single unit; thereby providing a fixed sample volume as the x component of ion velocity, $V_{ix}(x_o,y)$, is measured as a function of y position. $V_{ix}(x_o,y)$ is determined by measuring the frequency shift of the measured ion velocity distribution function (ivdf) relative to the natural frequency of the absorption line. Statistical uncertainty in the fits to the ivdf and iodine cell measurement limit the precision of the velocity measurement to ±50 m/s. During horizontal scans, the distance between the collection optics and injection beam remains fixed and the collection spot is scanned along the collimated laser beam; thereby providing a measurement of $V_{ix}(x,y_o)$.

The linear polarizer in the injection optics reduces the injected laser intensity by a factor of 2. However, by only pumping the π transitions ($\Delta m=0$) in the Ar-II $3d^2G_{9/2}$ to $4p^2F_{7/2}$ transition sequence, the much larger Zeeman splitting of the σ transitions ($\Delta m\pm1$) lines are avoided and the ivdf can be fit with a single thermally broadened Gaussian function. The internal Zeeman splitting of the π lines, Stark broadening, the natural linewidth of the absorption line, and the laser linewidth are ignorable. Ivdf width measurements, i.e., ion temperature measurements, obtained over the full range of available laser power indicate that power broadening due to saturation of the absorption line[15] is ignorable for the measurements reported here.

Measurements of $V_{iy}(x,y)$ are obtained by simply exchanging the injection and collection optical fibers on the 2D scanning apparatus. Because the collection optics do not include a linear polarizer, all three of the Zeeman split line clusters (π and 2σ) will contribute to the LIF signal and extraction of the y component of the ion temperature requires somewhat more sophisticated analysis. However, the bulk ion flow is still easily determined from the frequency shift in the measured ivdf. In addition to measurements of $V_{ix}(x,y)$ and $V_{iy}(x,y)$, measurements of $V_{iz}(x,y)$ are obtained by injecting the laser through a window at the right end of the source as shown in Fig. 1. For parallel injection, an Oriel™ circular sheet polarizer is used to convert the unpolarized laser light exiting the fiber optic cable into circularly polarized light. With the laser light of a single-circular polarization injected along the source axis, only one of the two σ transitions, specifically the $\Delta m=+1$ transition, is pumped. Using a single lens, the parallel optics produce a 0.8 cm diameter, collimated beam at the focal point of the collection optics mounted on the 2D scanning apparatus; yielding a sample volume of 6.3×10^{-3} cm^3. The parallel injection optics are attached to an optical mount that can be manually scanned along the y direction. The entire parallel assembly rests on another computer controlled Velmex™ stage that scans along the x direction. Thus, the parallel ivdf (and therefore the parallel ion flow) can be determined throughout the

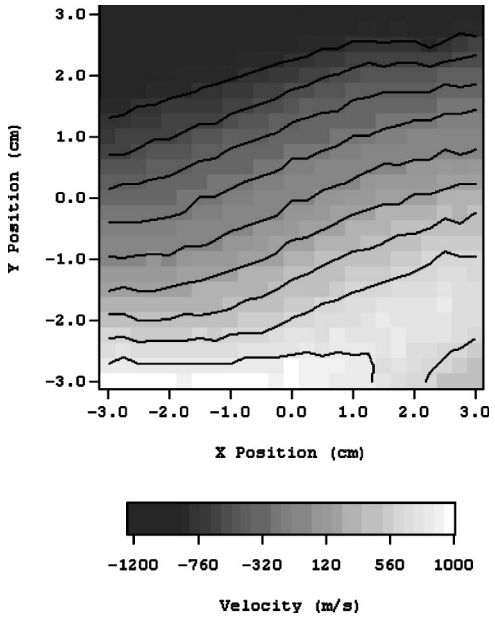

FIG. 3. Contours of constant $V_{ix}(x,y)$ in the center of the discharge for a source magnetic field of 652 G, rf power of 750 W, and a neutral pressure of 1.7 mTorr.

x, y plane for which the perpendicular flow measurements were obtained. Since the positioning errors for the stepping motors are much smaller than the injection and collection spot sizes, the spatial resolution of the flow field measurements is limited by the sizes of the perpendicular and parallel sample volumes.

III. OBSERVATIONS

The advantage of a complete cross section measurement of even a single velocity component is demonstrated with the $V_{ix}(x,y)$ plot shown in Fig. 3. If the plasma were rigidly rotating around the axis of source, the combined effects of projecting the rotational velocity along the x direction and the increase in tangential velocity with increasing radius would cancel and the measured $V_{ix}(x,y)$ values would be independent of x position, i.e., the contours of constant $V_{ix}(x,y)$ in Fig. 3 would appear as horizontal bars. The tilt to the contours in Fig. 3 can only be explained by a radially outward, diffusive, ion flow of 150 m/s. Although the same flow could be seen in a careful measurement of $V_{ix}(x,y=0)$, the precision in the flow measurements is comparable to the magnitude of the radial ion flow and it is the full 2D measurement that provides unequivocal evidence of the radially outward ion flow.

Shown in Fig. 4 for a vertical plane through the helicon discharge is the full 3D ion flow field overlaid atop the LIF intensity, proportional to the square of the metastable ion density in this collisional plasma,[16] for the same locations in the plasma. The bulk rotation of the plasma about the source axis is evident. Close inspection of the out of plane velocity component, the parallel velocity, indicates that parallel ion flow is largest at the edge of the plasma and decreases toward the plasma center. Thus, the ions in these helicon plasmas diffuse radially outward while rotating azimuthally at an angular frequency of roughly 36×10^3 rad/s and flowing toward the LEIA chamber with a peak parallel flow speed of 320 m/s at the plasma edge. The LIF intensity measurements indicate that the plasma density peaks slightly off axis ($x=-0.75$ cm,$y=0.5$ cm) and that the density profile is strongly peaked (see Ref. 16 for a complete discussion of the relationship between LIF signal intensity and plasma density in helicon sources).

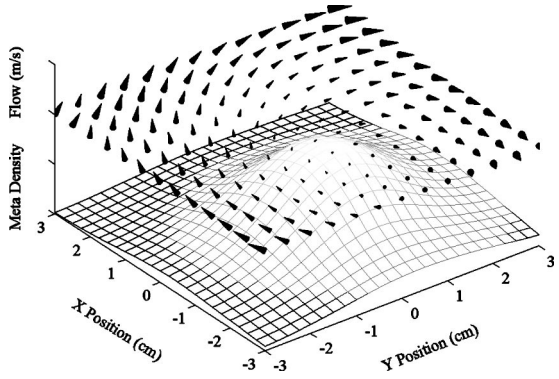

FIG. 4. The 3D ion flow field (vectors) and LIF signal intensity (contours) for the same plasma parameters used to obtain Fig. 3.

With additional Langmuir probe measurements of the ion density, electron temperature, and plasma potential radial profiles, all the terms of the complete momentum balance equation for ions in a cylindrical system can be determined. Initial analysis of the perpendicular flow measurements shown in Fig. 4 indicates that the observed ion flow field is consistent with expectations for $\boldsymbol{E}\times\boldsymbol{B}$ driven rotation (based on Langmuir probe measurements of $\boldsymbol{E}$) plus radial diffusion, i.e., the diamagnetic and second-order flow field divergence driven flows are ignorable.

ACKNOWLEDGMENTS

The authors thank Mike Zintl for providing the initial design of the 2D scanning apparatus and Rick Soulsby for the mechanical drawings used in its construction.

[1] R. A. Stern and J. A. Johnson III, Phys. Rev. Lett. **34**, 1548 (1975).
[2] R. A. Stern, D. N. Hill, and N. Rynn, Phys. Lett. A **93**, 127 (1983).
[3] D. N. Hill, S. Fornaca, and G. Wickman, Rev. Sci. Instrum. **54**, 309 (1983).
[4] J. M. McChesney, R. A. Stern, and P. M. Bellan, Phys. Rev. Lett. **59**, 1436 (1987).
[5] R. McWilliams and D. Sheehan, Phys. Rev. Lett. **56**, 2485 (1986).
[6] D. A. Edrich, R. McWilliams, and N. S. Wolf, Rev. Sci. Instrum. **67**, 2812 (1996).
[7] E. E. Scime, P. A. Keiter, M. W. Zintl *et al.*, Plasma Sources Sci. Technol. **7**, 186 (1998).
[8] A. D. Bailey III, R. A. Stern, and P. M. Bellan, Phys. Rev. Lett. **71**, 3123 (1993).
[9] F. M. Levinton and F. Trintchouk, Rev. Sci. Instrum. **72**, 898 (2001).
[10] M. Landerman, Senior Honors thesis, Swarthmore College, Swarthmore, PA, 2003, p. 84.
[11] M. Yamada, H. Ji, S. Hsu *et al.*, Phys. Rev. Lett. **78**, 3117 (1997).
[12] W. M. Ruyten and D. Keefer, AIAA J. **31**, 2083 (1993).
[13] E. E. Scime, P. A. Keiter, M. M. Balkey *et al.*, Phys. Plasmas **7**, 2157 (2000).
[14] I. D. Sudit and F. F. Chen, Plasma Sources Sci. Technol. **3**, 162 (1994).
[15] M. J. Goeckner, J. Goree, and T. E. Sheridan, Rev. Sci. Instrum. **64**, 996 (1993).
[16] X. Sun, C. Biloiu, R. Hardin *et al.*, Plasma Sources Sci. Technol. **13**, 359 (2004).